Ana Catarina Sousa Lobo

IMPACT OF PHOTODYNAMIC THERAPY WITH THE PHOTOSENSITIZER REDAPORFIN IN DISTANT METASTASIS

Master in Medicinal Chemistry

Chemistry Department

FCTUC

September, 2015

UNIVERSIDADE DE COIMBRA

Ana Catarina Sousa Lobo

IMPACT OF PHOTODYNAMIC THERAPY WITH THE PHOTOSENSITIZER REDAPORFIN IN DISTANT METASTASIS

Dissertation presented as evaluation for the Master in Medicinal Chemistry

Supervisor: Prof. Luis G. Arnaut

Co -Supervisor: Dr. Lígia C. Gomes-da-Silva

September, 2015

Universidade de Coimbra

« Porque eu sou do tamanho do que vejo, e não do tamanho da minha altura... »

Alberto Caeiro

Heterónimo de Fernando Pessoa

Para os meus pais, Céu e Luís

Sentes que um tempo acabou
Primavera de flor adormecida
Qualquer coisa que não volta, que voou
Que foi um rio, um ar, na tua vida

E levas em ti guardado
O choro de uma balada
Recordações do passado
O bater da velha cabra

Capa negra de saudade
No momento da partida
Segredos desta cidade
Levo comigo p'ra vida

Capa negra de saudade
No momento da partida
Segredos desta cidade
Levo comigo p'ra vida

Sabes que o desenho do adeus
É fogo que nos queima devagar
E no lento cerrar dos olhos teus
Fica esperança de um dia aqui voltar

E levas em ti guardado
O choro de uma balada
Recordações do passado
O bater da velha cabra

Capa negra de saudade
No momento da partida
Segredos desta cidade
Levo comigo p'ra vida

Capa negra de saudade
No momento da partida
Segredos desta cidade
Levo comigo p'ra vida

Balada da despedida do 5º ano jurídico de 88/89

AGRADECIMENTOS

Ao fim de cinco anos de aprendizagem, desafios e vivência académica, não posso deixar passar este momento sem agradecer àqueles que mais contribuíram para que tudo isto se tornasse possível.

Ao meu orientador, o Professor Doutor Luis Arnaut, pelo apoio científico, pela contribuição para o desenvolvimento deste projeto e pela constante motivação. Agradeço o desafio proposto de desenvolver este projeto, que me proporcionou um enorme crescimento a nível académico mas também a nível pessoal.

À Doutora Lígia Gomes-da-Silva, pelo conhecimento, determinação, energia e paixão pela ciência. Sinto um enorme orgulho e privilégio em ter iniciado o meu percurso científico sob orientação de alguém que me despertou ainda mais o gosto pela ciência, mostrando que pelo conhecimento e pela ciência não existem limites, e que há sempre algo mais que possamos fazer. Apesar da distância neste último ano, a sua contribuição e acompanhamento ao longo deste projeto foram fundamentais.

A todo o grupo de Estrutura, Energia e Reatividade que me acolheram de uma forma única. Ao Mestre Hélder Soares e ao Doutor Fábio Schaberle, por todo o acompanhamento no desenvolvimento deste projeto, pelas discussões científicas que em muito me fizeram crescer a nível científico mas também pessoal. Em muito agradeço este estímulo de querer idealizar sempre mais além do aquilo que esperam de nós. À Mestre Kamila Mentel, pela motivação e pela personalidade genuína, que sempre criou um ambiente alegre e agradável, mesmo nos momentos mais críticos.

Às grandes amizades que se construíram durante estes anos em Coimbra e que decerto permanecerão para a vida. Ao Alexandre Silva, à Ana Mata e à Joana Campos, colegas e amigos de laboratório, que nestes últimos dois anos me acompanharam de forma mais próxima, agradeço todo o apoio, conselhos, ideias e possibilidade de desabafo. A vossa companhia diária contribuiu imenso para o desempenho deste projeto. Obrigada por cada momento que passámos juntos, fosse em laboratórios, congressos ou convívios. À Ana Rita Ferreira, à Sara Antunes, à Carolina Vinagreiro e à Vanessa Tomé, um especial agradecimento por todo o tempo que passámos juntas. Pela partilha de conhecimentos e incertezas ao longo destes cinco anos de estudos, mas também pelos jantares e serões dos quais irei sentir imensa saudade.

Um especial agradecimento à Luzitin, SA, por fornecer a redaporfin e tornar possível todo o desenvolvimento deste projeto.

À Dra. Célia Gomes, por todo o acompanhamento nos procedimentos de imaging e por toda a disponibilidade, paciência e simpatia manifestada.

À Susana, pela amizade sincera, pela paciência e pela companhia a cada momento. A constante presença, mesmo que à distância, foi essencial e em muito contribuiu para alcançar esta etapa marcante no meu percurso académico. Obrigada por tudo.

Às minhas irmãs, Raquel e Andreia, pela amizade e cumplicidade. Apesar de distantes sempre senti a vossa presença e preocupação em cada etapa deste percurso. Sempre foram um apoio indispensável e a vossa boa disposição sempre me fizeram sorrir mesmo nos momentos mais difíceis. Obrigada pelo carinho.

Em especial aos meus pais, Céu e Luís, pelo amor, carinho e suporte ao longo de todo este percurso. O esforço e dedicação que por mim fizeram ao longo destes anos foram fundamentais para o meu crescimento pessoal e académico. São para mim um exemplo de coragem e um dos meus grandes orgulhos.

Por fim, não posso deixar de agradecer à cidade que me acolheu nestes últimos 5 anos: a Coimbra. Uma cidade repleta de cultura e tradições, que nos envolve e acolhe os estudantes de uma forma única.

Saudade é o sentimento que fica após um ciclo de cinco anos de sonhos, algumas frustrações, mas sobretudo vivências intensas e memoráveis.

Impact of Photodynamic Therapy with the photosensitizer redaporfin in distant metastasis

Ana C. S. Lobo*[1], Lígia C. Gomes-da-Silva[1], Célia M. Gomes[2] and Luis G. Arnaut[1]

[1] Chemistry Department, University of Coimbra, Rua Larga, 3004-535 Coimbra, Portugal

[2] IBILI, Faculty of Medicine, University of Coimbra, Azinhaga de Santa Comba, 3000-354 Coimbra, Portugal

KEYWORDS: Photodynamic Therapy, redaporfin, cancer, metastasis, immune system, metastatic animal model, photodynamic immunotherapy, treatment optimization

ABSTRACT: Metastatic diseases are the main cause of death of cancer patients. Thus, treating cancer disease requires therapies capable of treating primary tumors but also able to eradicate distant secondary diseases. Photodynamic therapy (PDT) with redaporfin has revealed promising results, with high percentage of cures of subcutaneous tumors along with the ability to stimulate the immune system. Our purpose was to develop a protocol for an animal model (BALB/c mice with orthotopic 4T1 mammary carcinoma tumor) that can be used to compare surgery against PDT in the elimination of the primary tumor and the control of metastasis. BALB/c mice were inoculated with different number of 4T1-luc2 cells in the abdominal mammary gland. The tumor kinetics was followed to assess the onset of metastatic disease by bioluminescence imaging. The first detection of metastases in the animals subjected to surgery was observed 27 days after inoculation. The higher percentage of metastization corresponded to the inoculation of $2x10^4$ cells. The resistance of 4T1 tumors and the location of the tumor are a challenge to PDT. The optimization of PDT with redaporfin proved difficult to treat and may require new strategies capable of potentiate PDT impact on the primary tumor and minimize the adverse effects in the surrounding healthy tissues, thus enabling the evaluation of potential effects in distant metastasis.

ABBREVIATIONS

PDT, photodynamic therapy; PS, photosensitizer; ROS, reactive oxygen species; F_2BMet (or redaporfin), 5,10,15,20-tetrakis(2,6-difluoro-3-N-methylsulfamoylphenyl)bacteriochlorin; HPD, hematoporphyrin derivative; DLI, drug-to-light interval; ECM, extracellular matrix; BLI, bioluminescence imaging; Tregs; regulatory T cells; IL6, interleukin 6; APC, antigen-presenting cells.

INTRODUCTION

Photodynamic therapy (PDT) is a treatment modality based on 3 essential components which are individually nontoxic: photosensitizer (PS), light and oxygen. The photosensitizer is administrated either systemically, locally or topically to a patient bearing a lesion, frequently a cancer disease, followed by irradiation of the lesion at a wavelength corresponding to an absorbance band of the PS. This illumination in the presence of oxygen leads to the generation of cytotoxic species and consequently leads to a series of events that cause direct tumor cell death, damage to the microvasculature and induce a local inflammatory reaction[1,2].

The PS in the ground state has its electrons populating the lowest energy molecular orbitals. The two electrons populating each orbital have opposite spins, hence the ground state of the PS is a singlet state (S_0). After the absorption of light one of these electron is boosted into a high-energy orbital originating the first excited singlet state (S_1). This is a short-lived (nanoseconds) species that can lose its energy by emitting light by fluorescence or by radiationless transitions into heat. The S_1 state of PS can undergo intersystem crossing whereby the spin of the excited electron inverts to form a relatively long-lived (microseconds) excited triplet-state (T_1) that has two electrons with the same spin in the two highest singly occupied molecular orbitals. This T_1 state may undergo two different pathways: in type 1 reactions it can react directly with a substrate or with oxygen and transfer a proton or an electron to form a radical; in type 2 reactions the triplet state of the PS can transfer its energy directly to the molecular oxygen to form excited-state singlet oxygen[3].

The radical species generated, such as the superoxide ion ($O_2^{\cdot-}$), may produce other reactive species such as H_2O_2 or $HO^{\cdot}$ in biological media, which together with the singlet oxygen from type 2 reactions are designated reactive oxygen species (ROS). ROS are oxidizing agents that can react with many biological molecules, including the DNA. Although cells have some capability of repairing oxidative damage, excessive impairment can cause mutations and lead to cell death. However, due to the high reactivity and short half-life of these species, oxidative damage only affect molecules close to the volume of ROS production (volumes of PS localization).

How light spread in the target tissue may also have different impacts in PDT efficacy, as it can be absorbed or scattered when it enters tissue, depending on tissue type and light wavelength. Due to the absorption of important tissue chromophores like oxy, deoxyhemoglobin and melanin at the visible and the occurrence of water absorption at wavelengths greater than 1300 nm, the optimum wavelength window in tissue occurs between 600-800 nm, known as the phototherapeutic window[3]. Usually as the PS is a fluorescent and photochemically active molecule, both imaging and detection strategies can be applied in PDT protocols. This dual function is an advantage.

Characteristics of the ideal PS have been extensively described over the last years. PS should have low dark toxicity, absorb light in the red or far-red wavelengths (600-800 nm), where tissues have higher optical penetration (δ= 2.3 mm at 750 nm)[4], and high absorption bands to minimize the dose of PS needed to achieve the desired effect. The ideal PS should have a simple synthesis, be a pure compound, have a long shelf-life and a relatively rapid clearance from normal tissues to minimize the phototoxic side effects. Other desirable properties of PS agents have been described in literature[1,3,5–7].

The time elapsed between PS administration and tumor illumination, known as drug-to-light interval (DLI), influences the location of the PS and can be a critical component of controlling PDT. Vascular therapy is a PDT modality that involves the irradiation of the tumor area less than 30 minutes after compound administration, meaning that the PS is still on the vasculature and originating damages in vessels.[1] With short DLI protocols, the clearance effects are still minimal, requiring lower doses to achieve the desired effect (improved cost-effectiveness) when compared with higher DLI intervals. The administration of PS with larger DLI (such as 72h), which enables the compound to accumulate inside or nearby cancer cells, are designated as cellular protocols[5].

The adverse effects reported for PDT are related to the long-lasting photosensitivity, pain during some treatments protocols and excessive healthy tissue destruction at the treated area[1,3].

The majority of the PS are based on tetrapyrrole macrocycle found in natural occurring pigments such as heme chlorophyll and bacteriochlorophyll. Tetrapyrrole macrocycles usually have a relatively large absorption band in the region of 400 nm known as the Soret band, and a set of progressively smaller absorption bands at longer wavelengths known as the Q-bands. Porphyrins have the longest wavelength absorption bands in the region of 630 nm but these tend to be weak. Chlorins are tetrapyrroles with the double bond in one pyrrole ring reduced, which shifts the longest wavelength absorption band to the region of 650-690 nm and increases several folds the absorptivity. Both these factors are highly desirable for PDT. Bacteriochlorins have the absorption band shifted even further into the red and increased further in magnitude due to the two pyrroles rings with reduced double bonds[3].

The first PS to be clinically employed for cancer therapy was hematoporphyrin derivative (HPD), a purified form of which, porfimer sodium, was later commercialized as Photofrin[8]. Although porfimer sodium is still the most widely employed PS, it has some disadvantages such as the long-lasting photosensitivity and the relatively low absorbance at 630 nm. There have been major efforts among scientists to develop second-generation PSs and several hundreds have been proposed as potential PS for anticancer PDT[1].

Temoporfin is a chlorin photosensitizer characterized by long plasma half-lives ($t_{1/2}$ = 45.4 h) and is prescribed with drug-to-light intervals of 4-6 days. This favors higher tumor selectivity but also prolonged skin photosensitivity[9,10]. Verteporfin is another photosensitizer that has been licensed for the treatment of age-related macular degeneration which is characterized by a reduced period of photosensitivity ($t_{1/2}$ = 5-6 h) when compared with temoporfin. Verteporfin is currently in clinical trials on pancreatic cancer[11,12].

Redaporfin is a photostable bacteriochlorin with intense infra-red absorption, high yield of ROS generation, high phototoxicity, low skin photosensitivity and favorable pharmacokinetics[13,14]. The optimized PDT treatment regime leads to significant long-term survival rates, with 86% cure rate in BALB/c mice with subcutaneously implanted CT26 tumors, but no cures in BALB/c nude mice with the same tumor model, revealing the significance of the immune system.

The result of the oxidative stress from PDT treatments gives a mixture of apoptotic and necrotic cell death and the balance among different cell death pathways is dependent of several PDT parameters, such as the total PDT dose, the drug dose, the oxygen concentration, the cell type and the localization of the PS inside tumor cells. This oxidative stress usually induces immune modulation effects, such as the expression of tumor antigens, shortly after the treatment, characterized by a strong acute inflammation localized in the treated area[2]. This acute inflammatory response results in an influx of various immune cells, such as neutrophils, immature dendritic cells and macrophages into the injured area, which are responsible for ensuring the removal of the damaged cells and promoting local healing[15,16]. Although, in part, this is a tumor antigen nonspecific response by the innate immune system, many studies have demonstrated that PDT may induce multiple danger signals capable of triggering antigen-presenting cell (APC), such as B cells, macrophages and dendritic cells. APC became activated and then trigger T lymphocytes through presentation of tumor antigens. This activation may elicit an adaptive immune antitumor effect responsible for eliminating surviving cancer cells escaped to the direct effects of PDT but also other distant cancer cells[1,2,17,18]. Thus, in response to the treatment, cancer cells die triggering a tumor-specific immune response and this is designated as immunogenic cell death.[18]

Evidence that local PDT with redaporfin can have systemic effects has been found in many experiments: cured mice rechallenged over 3 months later with CT26 rejected the tumor cells in 67% of the cases[19]; it was observed an antitumor effect in a second untreated tumor in an animal bearing two distant tumors after the treatment of one of them; and the stimulation of the immune system that was recently confirmed, revealing an increase of neutrophils number and secreted cytokines after treatment (unpublished data). PDT with redaporfin also reduced lung metastasis in a pseudo metastatic model, when mice with subcutaneous CT26 tumors where treated 5 days after the additional intravenous injection of CT26 cells[19]. Redaporfin is currently in clinical trials on advanced head and neck cancer (ClinicalTrials.gov Identifier: NCT02070432).

Metastasis are the main cause of death in cancer patients, more than 90% of cancer deaths are the result of metastasis[20]. Thus, treating cancer disease requires therapies capable of treating primary tumors but also able to eradicate distant secondary diseases[21].

The metastatic process is an extremely complex process and is presumed that only a small fraction of tumor cells have the ability to metastasize. Metastasization consists in the detachment of epithelial cells from the extracellular matrix (ECM), infiltration in the blood and/or lymphatic system, survival and growth at the metastatic site[22].

This work intends to develop a protocol for an animal model that can be used to compare surgery against PDT in the elimination of the primary tumor and control of metastasis. In this study we used the poorly immunogenic BALB/c-derived mouse mammary carcinoma, 4T1, which mimics the human stage IV breast cancer in its immunogenicity, metastatic properties and growth characteristics. 4T1 tumors are highly aggressive and spontaneously metastasize throughout the body, in a pattern similar to human breast cancer, to lymph nodes, lungs, liver, brain, blood and bone [23–27].

EXPERIMENTAL SECTION

MATERIALS AND METHODS

Chemicals

5, 10, 15, 20-Tetrakis(2, 6– difluoro- 3– N– methylsulfamoylphenyl)bacteriochlorin (F_2BMet or redaporfin) was recently described[14]. Luzitin SA (Coimbra, Portugal) provided redaporfin as a powder in a sealed amber glass vial under N_2 atmosphere. D-Luciferin was purchased from Caliper Life Sciences. Details on drug formulations are presented in Supplementary Materials.

Cell lines and cell culturing

4T1 and 4T1-luc2 cell lines were purchased from ATCC and Perkin Elmer, respectively, and were maintained in RPMI medium 1640 supplemented with 10% fetal bovine serum, 1% penicillin/streptomycin at 37°C in 5% CO_2 and 95% humidity. 4T1-luc2 is a luciferase expressing cell line which was stably transfected with firefly luciferase gene (luc2) and allows to access the metastasis onset in animal models with bioluminescence imaging (BLI). All reagents were purchased from Sigma Life Sciences unless stated otherwise.

In vitro PDT treatments

From 4T1 and 4T1-luc2 cell lines, cells were seeded into 96-well plate at a cell density of 6000 and 7000 cells/well, respectively. After 24 h redaporfin was administered to both cell lines at several concentrations, from 0.075 to 10 μM. After an incubation period of 20 h cells were washed 3 times with PBS and, immediately after, cells were irradiated with a light emitting diode, LED, (750±20 nm) with a light dose of 0.1 J/cm^2. In order to evaluate the viability it was performed the Alamar blue assay 24 h after LED irradiation. Details on Alamar blue protocol are presented in Supplementary Materials.

In vitro PDT treatments in the presence of anesthesia

4T1 cells were seeded at a cell density of 7000 cells/well and 24 h after plating, cells were incubated with redaporfin alone and with different concentrations of anesthesia (a mixture of ketamine: xylazine in 5:1 ratio), in ratio w:w. After an incubation period of 20 h cells were washed 3 times with PBS and, immediately after, cells were irradiated with a light emitting diode, LED, (750±20 nm) with a light dose of 0.1 J/cm^2. In order to evaluate the viability it was performed the Alamar blue assay 24 h after LED irradiation.

Metastatic Animal Model Optimization

Female BALB/c mice were obtained from Charles River Laboratories® (Barcelona, Spain) and were used with 9 to 12 weeks of age, weighing 18-24 grams. Before each tumor inoculation, all of the hair in the mammary gland region was removed with depilatory cream. For metastatic model optimization, different number of 4T1-luc2 cells which were taken up in 0.05 mL of RPMI without serum and antibiotics ($1x10^4$, $2x10^4$, $5x10^4$ and $10x10^4$ cells) and were orthotopically transplanted into the abdominal mammary gland of each animal. Before inoculation animals were anesthetized with a mixture of ketamine/xylazine (5:1), 120 mg/kg and 10 mg/kg, respectively. Tumor size was measured with calipers bi-weekly once tumors became palpable and mean tumor volume was calculated with the formula $(a \times b^2)/2$, *a* referring to the largest and *b* to the shortest diameter of the tumor. Animals were submitted to surgery when the tumor diameter reached 4 mm. BLI of live animals was initiated at 27 days after cell line injection and performed weekly until day 41, and then animals were sacrificed.

Mouse Tumor Model

For the tumor establishment $2x10^4$ 4T1-luc2 cells were taken up in 0.05 mL of RPMI without serum and antibiotics and were orthotopically transplanted into the abdominal mammary gland of each animal. Tumor size was measured with calipers bi-weekly once tumors became palpable and mean tumor volume was calculated with the formula $(a \times b^2)/2$. Primary tumors were treated 7-11 days after the inoculation when tumor diameter reached 4-5 mm. Control animals were submitted to surgery and animals were sacrificed when the tumor diameter reaches 8-10 mm or when mice became moribund (i.e., weight loss > 20%, visible prostration).

PDT regimens

Tumor illumination protocols described in Table 1 used a continuous wave (CW) laser with emission at 749 nm supplied by Omicron which was handled close to the surface of the tumor with a specific diameter of the laser spot. Tumor dimensions were determined before the illumination.

In vivo luminescence imaging

Detection of metastasis by bioluminescence imaging (BLI) was performed using a charge-coupled device camera–based bioluminescence imaging system (IVIS Lumina XR, Caliper Life Sciences, Hopkinton MA; exposure time 1–300 sec, binning 8, field of view 4-23 cm). Before image acquisition, all of the hair in the frontal region was removed with depilatory cream. After the mice were anesthetized with a mixture of ketamine/xylazine (5:1), 120 mg/kg and 10 mg/kg, respectively, D-luciferin potassium salt (150 mg/kg) were intraperitoneally injected to the mice 5 minutes prior to imaging acquisition. Signal was measured and recorded as total flux (photons/sec) and data was analyzed with Living Image software (Caliper Live Sciences).

Statistical Analyses

All of the measured values are presented as mean ± SD. Statistical analyses were performed using Prism v. 4.5 (GraphPad Software). Data were analyzed with unpaired two-tailed Student's t tests or one-way analysis of variance (ANOVA) tests as indicated in respective figure legends. Details on statistical data are presented in Supplementary Materials.

RESULTS

In vitro PDT treatments – Cell lines comparison

In order to evaluate if there were any significant differences between in vitro PDT treatments in parental and transfected cells, PDT treatments were performed in both cell lines, 4T1 and 4T1-luc2, with a range of concentrations of redaporfin to compare the

IC50 value for each cell line. From our results, IC50 value for 4T1 cell line is 1.3 ± 0.4 μM and for 4T1-luc2 cell line is 1.1 ± 0.3 μM. Although apparently it seems to exist some differences in the manipulation and fragility of 4T1-luc2 when compared to 4T1, differences between the IC50 values were not statistically significant using a unpaired two-tailed Student's t test with P> 0.05 (p = 0.6). On the other hand, when compared with other cell lines the IC50 of mammary carcinoma cell line is relatively lower, indicating that this tumor cell line appeared to be more vulnerable in vitro when compared to other cancer lines undergoing PDT[14].

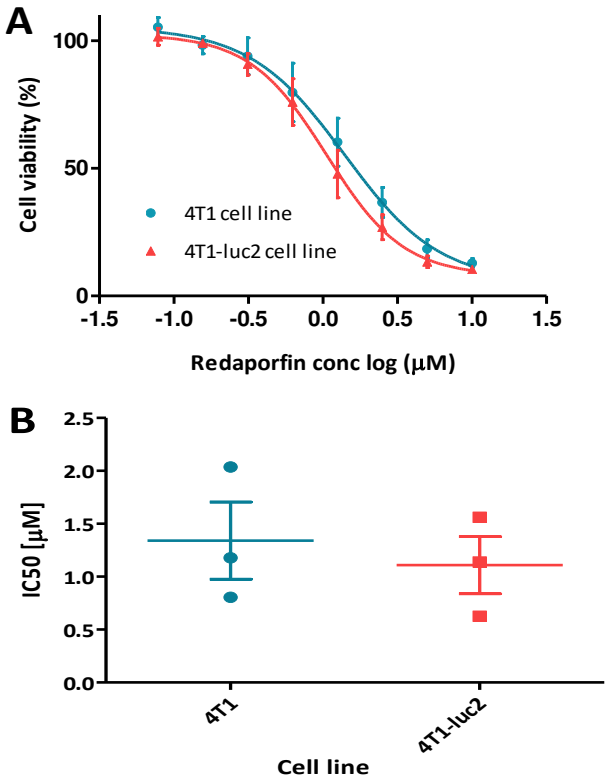

Figure 1. Data from in vitro PDT treatments with redaporfin. **A** Dose-response curves of 4T1 and 4T1-luc2 cell lines to PDT treatments with different concentrations of redaporfin. **B** IC50 values for each cell line which reveal no statistical differences between cell lines vulnerability to redaporfin PDT. The statistical significance of data the Student's t test was performed at a P set at 0.05 (p=0.6).

Metastatic Animal Model

Classical orthotopic models are impractical for evaluation of treatment's efficacy since they require large numbers of animals to be sacrificed at each time point. The cell line used in this work was transfected with firefly luciferase gene (luc2) which allows to follow the metastasis onset and growth without sacrificing the animals.

To confirm the metastatic potential of 4T1 mammary carcinoma and to optimize a metastatic model capable of comparing metastasization after surgery and after PDT treatment, mice were challenged with different number of cancer cells and metastasis establishment was assessed after animals were subjected to surgery.

Since the number of inoculated cells affects the onset and kinetics of tumor growth, animals were submitted to surgery when the largest diameter of the tumor attained 4 mm, between 7 and 17 days after the cell inoculation, as is schematized in Figure 2. Metastasization was monitored by bioluminescent imaging between days 27 and 41, and then the animals were sacrificed.

The first detection of metastases in animals subjected to surgery was observed 27 days after inoculation (Supplementary Information) and the higher percentage of metastasization (75%) corresponded to the inoculation of $2x10^4$ cells (Figure 3).

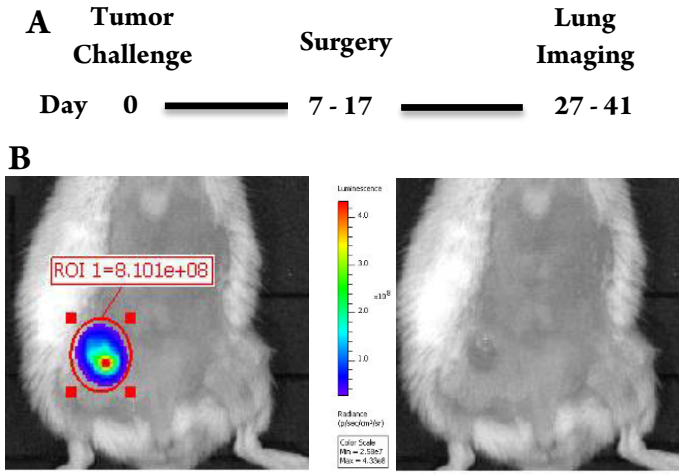

Figure 2. Overview of metastatic model optimization. **A** Schematic outline of metastatic model optimization protocol: Different number of cells were inoculated in the mammary gland ($1x10^4$, $2x10^4$, $5x10^4$ and $1x10^5$ cells) and surgery was performed when tumor diameter attained 4 mm. Lung imaging was performed on days 27, 34 and 41. **B** IVIS image and photograph of 4T1-luc2 mammary carcinoma tumor ($2x10^5$ inoculated cells) at day 14 (IVIS acquisition settings: exposure time 2 sec, binning 4, field of view 10 cm).

In vitro PDT treatments in the presence of anesthesia

Previous PDT protocols with redaporfin always involved irradiation of the tumor in the animal thigh, and the illumination of tumors could be performed while animals were maintained motionless by the investigator. However, in the animal model studied in this work, the inoculation of the tumor is in the abdominal area, the irradiation may cause some discomfort on the animal and it could be very difficult to keep the animal motionless. The motion of the animal during the treatment may have a major impact in PDT efficacy. The movement of the animal may change spot of irradiation and light scattering and therefore the total dose of light delivered to the target tissues. This may reduce the impact of PDT on the tumor and increase damage to the adjacent healthy tissues. Thus, it was necessary to anesthetize animals before the irradiation procedure.

In vitro PDT treatments in the presence of anesthesia were required to confirm that anesthesia would not have an antioxidant effect during PDT treatments, as it is suggested with some anesthetic drugs[28,29], that could protect cancer cells from cytotoxic effects of PDT and could justify preliminary results with no impact in 4T1 tumors after treatments. From our results in Figure 4 it was demonstrated that the presence of anesthesia from high to low concentration during in vitro PDT protocols do not affect the efficacy of PDT. In fact, the presence of anesthesia in higher concentrations apparently seems to have some synergetic cytotoxic effect with redaporfin. However, these differences were not statistical significant.

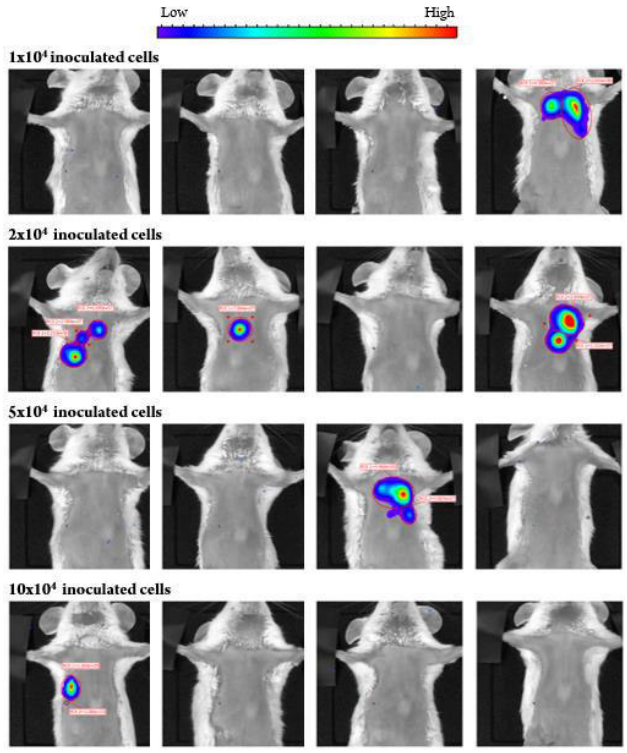

Figure 3. Detection of lung metastasis in vivo. Assessment of lung metastasis was performed by bioluminescent imaging. D-luciferin was injected 5 min prior to images acquisition and bioluminescent images were taken using an IVIS Lumina XR. Data refers to imaging 41 days after tumor inoculation. Higher percentage of metastasization was obtain with the inoculation of $2x10^4$ cells, corresponding to 75 % of metastasized animals.

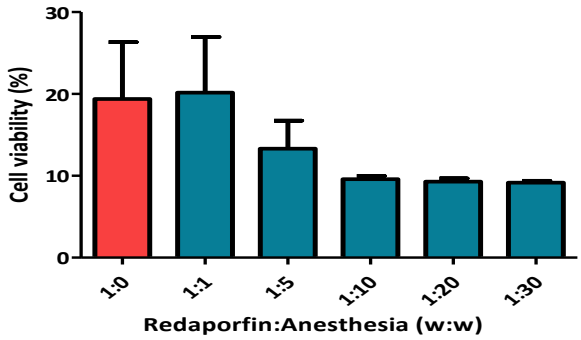

Figure 4. Data from in vitro PDT treatments in 4T1-luc2 cell line in the presence of anesthesia. Cells were incubated with 5 μM redaporfin alone and with different concentrations of anesthesia, ratio (w/w), (20 h incubation) which revealed no statistical differences when compared with PDT with redaporfin alone. To evaluate the statistical significance of data the one-way ANOVA followed by Dunnett's Multiple Comparison test was performed at a P set at 0.05.

In vivo PDT regimens

The optimization of PDT protocol was initiated with the optimized PDT parameters for CT26 tumor model, Protocol 1 in Table 1, which was described recently[19] and offered 86 % cure rate in BALB/c mice. However, in the orthotopic mammary carcinoma model these conditions revealed to be potentially lethal and with no impact on tumors. Necropsies of animals submitted to this protocol revealed major impact in the adjacent healthy tissues: liver, kidney and small intestine.

The following protocols resulted in changes in drug dose and in diameter of irradiation, but still with no impact on the tumors. Combinatory therapies were introduced to reduce the vascular doses of PS (with DLI of 0.25 h) and were sequentially replaced by cellular doses (with DLI of 72h), which could enabled higher dosage of PS and achieve a more localized treatment. Although many regimens were explored balancing light and PS dose this optimization was not successful in means of achieving an effective treatment capable of eradicate or reduce the tumor kinetic growth. The greatest impact on tumors was obtained through protocol 9 that led to necrosis in the surface of the tumors after 48-72 h, however tumors started to regrowth after 72h (Figure 5). The kinetics of tumor growth of protocol 9 and 11 in comparison with a control group (with no treatment) are represented in Figure 6.

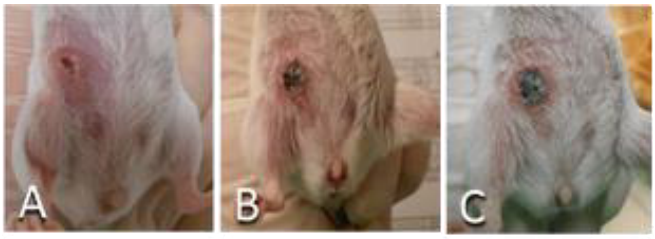

Figure 5. Impact of PDT of protocol 9, described in Table 1. A - before PDT; B – 24 h after PDT; C – 48 h after PDT. Tumor regrow 72 h after PDT.

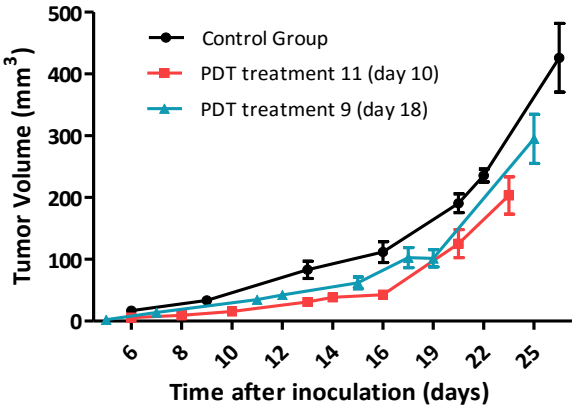

Figure 6. Kinetics of 4T1 tumor growth: comparison between control group (animals submitted to no treatment), PDT protocol 9 (treatment on day 18) and PDT protocol 11(treatment on day 10).

DISCUSSION

The 4T1 tumor is highly invasive and develops spontaneous metastasis from the primary tumor. In comparison with the clinical situation, the primary tumor can be surgically removed and the metastatic foci remains intact, so the metastatic disease can be studied in animal models[24]. Non-invasive whole body bioluminescence imaging allows repeated, real-time in vivo monitoring of tumor growth in experimental animals, regardless of tumor locations adding advantages over traditional models.

Table 1. Studies of PDT regimens for 4T1-luc2 orthotopic tumor illumination protocol optimization.

Protocol	Drug-to-light interval (DLI)(h)	Drug dose (mg/kg)	Light dose (J/cm^2)	Laser Power (mW)	Diameter (cm)	Survivals to the treatment (%)	Impact on the tumor
1	0.25	1.00	50	173	1.3	43	no impact
2	0.25	0.75	50	173	1.3	100	no impact
3	0.25	0.75	50	173	1.1	100	no impact
4	0.25	1.00	50	173	1.1	100	no impact
5	72	1.00	100	173	1.3	100	necrosis
6	72 & 0.25	1.00 & 0.5	80	173	1.3	0	-
7	72 & 0.25	1.00 & 0.5	60	173	1.3	100	no impact
8	24 & 0.25	1.00 & 0.5	50	173	1.0	0	-
9	144 & 72 & 0.25	1.00 & 1.00 & 0.4	50	173	1.0	100	necrosis
10	72 & 0.25	2.00 & 0.4	50	173	1.0	0	-
11	72	2.00	50	173	1.0	100	edema
12	72	2.00	75	103	1.0	0	edema and necrosis
13	72	2.00	65	103	1.0	0	edema

Our results from the metastatic model optimization showed that the inoculation of $2x10^4$ cells can originate metastasization in 75% of the cases, being able to be used as a metastatic model that mimics the human cases and allows non-invasive detection and quantification of metastasis in live animals as means of assessing drug/treatment efficacy. Our results confirmed that the inoculation of a smaller number of cells facilitates the metastization process, as it is mentioned in literature[24,30].

Vascular PDT with redaporfin found remarkably efficient in the treatment of CT26 tumors in animals' thigh[19]. Under these conditions the damages occur mainly in the vasculature of tumors and generating tumor hypoxia and starvation, which leads to tumor ablation and stimulation of the immune system. However, the optimized protocol for CT26 tumors did not give the same kind of results in 4T1 models, which originated 43% of treatment survival, and the animals that survived to the treatment revealed no impact on tumors. This results may be due to the fact of 4T1 tumors being described as highly vascularized tumors[15,24], thus, the protocol that leads to destruction of CT26 tumor vasculature may not be enough to cause the same effect in the robust vessels of 4T1 tumors.

The aggressive and invasive characteristics and the location of 4T1 tumors represents a challenge to PDT. The requisite of administering higher PS (redaporfin) and light doses to achieve a significant impact on the tumor, has the limitation of the tumor location in the abdominal region. The majority of the drugs have tendency to accumulate in liver and kidneys (elimination organs) and adverse effects of the treatment in adjacent vital organs, such as liver, kidneys and bowel may limit the survival of animals to the treatment.

Cellular protocols with DLI of 72 h which enables the compound to accumulate inside or nearby cancer cells, appeared to be more suitable than vascular methodologies. Although we verified some effects of PDT on tumors (edema and necrosis), the treatments were not effective and the adverse effects in the adjacent tissues still remained. The concentration of PS in organs of elimination is always higher than the accumulation in tumor[13] and can increase over time due to drug clearance effects. Excessive damages on vital organs may also occur mainly due to the small dimensions of BALB/c mice, in which the distance between organs and the irradiation spot is not sufficient to avoid these effects. This fact might be circumvented through the application of models with larger animals, such as the wistar rat model.

PDT efficacy is also limited by light fluence rate (irradiance) of tumor illumination. High fluence rates may originate photobleaching of PS and high percentages of singlet oxygen formation leading to oxygen consumption. This excessive consumption may decrease the PDT efficacy since volume of oxygenated and therefore PDT-sensitive tissue are reduced. On the other hand, low fluence rates may remain at the sub-lethal damage levels and originate ineffective treatments[19,31].

Irradiations with a diameter spot greater than the size of the tumor is important to the effectiveness of the treatment as it inhibits the resupply of nutrients to the tumor. On the other hand, the increase of the irradiation spot can lead to excessive destruction of adjacent tissues. [19] During treatment optimization in this study, the spot of irradiation was diminished in order to minimize the adverse effects on adjacent tissues. However, the outcome of treatments did not improve.

A number of studies have also tried to obtain an effective treatments with 4T1 metastatic model, however outcomes were not satisfactory. Gollnick's group demonstrated a significant reduction of lung tumors in an experimental metastasis model with EMT6 mammary carcinoma cells, but the 4T1 metastatic model proved difficult to treat with PDT with Photofrin. Although, primary tumor repressed initially after PDT, it grew up in one week and spontaneous lung metastasis were not controlled with this treatment.[15] During these studies it was demonstrated that the number of regulatory T cells (Tregs) is significantly higher (≈ 3000 times) in 4T1 tumors rather than EMT6 tumors before PDT. This may suggests that Tregs may contribute to suppression of tumor response.[15] It has been also demonstrated that IL6 is a cytokine that has been shown to play a

major effect in T-cell proliferation, survival and function[32], and its production appears to be enhanced after PDT in 4T1 tumors. However, IL6 has been shown to potentiate tumor resistance and survival to PDT and to inhibit therapy enhancement of immune memory[33].

PDT treatments with redaporfin still need to be further optimized for this metastatic model, even though some of the barriers have been predicted. This experiments revealed essential evidences about 4T1 tumor responses to PDT treatment and several strategies may still be challenged with this cell line.

Frontal irradiation already revealed many limitations and the implementation of interstitial irradiation may circumvent some of them, such as the undesirable effects of light scattering in surrounding tissues and the need to ensure a homogenous illumination of all tumor bulk[34,35].

Combinatory therapies involving a large range of immunoadjuvants have been considered in literature as possible enhancers of PDT efficacy through the immune system stimulation[16,36]. Low dose cyclophosphamide is a traditional cytotoxic cancer drug that damages tumor DNA and has been recognized for inducing an antitumor immune response through the depletion of regulatory T cells[36–39], which are recognized as suppressors of immune system response and are highly present in 4T1 tumors after in immune-augmenting treatments in tumor bearing hosts[40].

Hamblin et al.[41] also used the 4T1 metastatic model to study PDT effects with Verteporfin. However, the results shown a relative lack of major tumor destruction by PDT alone. The combinatory therapy of PDT with CPG-ODN immunoadjuvant in turn had a bigger impact in the treatment of this model, with delay in the local tumor progression and a corresponding increasing in the survival.

Many other efforts have been applied to understand PDT mechanisms and to apply strategies to improve PDT impact. Our group have been involved in several studies with the purpose of increasing PS phototoxicity for instance through the inhibition of dismutase superoxidase (Mn-SOD), which may enhance the capacity of PS to transfer an electron to molecular oxygen and consequently enhancing PDT efficacy (unpublished data).

CONCLUSIONS

Photodynamic therapy with redaporfin had revealed promising results, particularly the ability to stimulate an antitumor immune response that is responsible for the effectiveness of the optimized protocol for CT26 models. However, the resistance of 4T1 cells and the location of the tumor are a challenge to PDT. Effective treatments requires new strategies capable of providing an improved impact on the primary tumor without generating excessive damage in the surrounding healthy tissues, thus enabling the evaluation of potential effects in distant metastasis.

AUTHOR INFORMATION

Corresponding Author

* Ana Catarina Sousa Lobo
catarinalobo13@gmail.com

Department of Chemistry, University of Coimbra
Rua Larga, 3004-535 Coimbra, Portugal

ACKNOWLEDGMENT

The Coimbra Chemistry Center is supported by the Fundação para a Ciência e a Tecnologia (FCT), Portuguese Agency for Scientific Research, through the project PTDC/QUI-QUI/120182/2010 and the project PEst-OE/QUI/UI0313/ 2014. We thank Luzitin SA for the gift of redaporfin. We grateful appreciate the help of Dr. Célia Gomes (IBILI-FMUC, Portugal) with the bioluminescence measurements. It is also acknowledge all the support from the Structure, Energy and Reactivity group, particularly Dr. Lígia Gomes-da-Silva and Professor Luis Arnaut for all the support and guidance provided along the realization of this project.

REFERENCES

(1) Agostinis, P.; Berg, K.; Cengel, K. a; Foster, T. H.; Girotti, A. W.; Gollnick, S. O.; Hahn, S. M.; Hamblin, M. R.; Juzeniene, A.; Kessel, D.; et al. Photodynamic Therapy of Cancer : An Update. *Am. Cancer Soc.* **2011**, *61*, 250–281.

(2) Castano, A.; Mroz, P.; Hamblin, M. Photodynamic Therapy and Anti-Tumour Immunity. *Nat. Rev. Cancer* **2006**, *6* (7), 535–545.

(3) Castano, A. P.; Demidova, T. N.; Hamblin, M. R. Mechanisms in Photodynamic Therapy: Part One - Photosensitizers, Photochemistry and Cellular Localization. *Photodiagnosis Photodyn. Ther.* **2004**, *1* (4), 279–293.

(4) Bashkatov, a N.; Genina, E. a; Kochubey, V. I.; Tuchin, V. V. Optical Properties of Human Skin, Subcutaneous and Mucous Tissues in the Wavelength Range from 400 to 2000 Nm. *J. Phys. D. Appl. Phys.* **2005**, *38* (15), 2543–2555.

(5) Allison, R. R.; Moghissi, K. Photodynamic Therapy (PDT): PDT Mechanisms. *Clin. Endosc.* **2013**, *46* (1), 24–29.

(6) Allison, R. R.; Downie, G. H.; Cuenca, R.; Hu, X. H.; Childs, C. J. H.; Sibata, C. H. Photosensitizers in Clinical PDT. *Photodiagnosis Photodyn. Ther.* **2004**, *1* (1), 27–42.

(7) Detty, M. R.; Gibson, S. L.; Wagner, S. J. Current Clinical and Preclinical Photosensitizers for Use in Photodynamic Therapy. *J. Med. Chem.* **2004**, *47* (16), 3898–3915.

(8) Kotoula, M. G.; Tsironi, E. E.; Karabatsas, C. H.; Chatzoulis, D. Z. Photodynamic Therapy. *Retina* **2005**, *25* (1), 102–103.

(9) Peng, Q.; Moan, J.; Ma, L.; Nesland, J. M. Uptake , Localization , and Photodynamic Effect of Meso -Tetra (Hydroxyphenyl) Porphine and Its Corresponding Chlorin in Normal and Tumor Tissues of Mice Bearing Mammary Carcinoma. *Cancer Res.* **1995**, *55*, 2620–2626.

(10) Andrejevic-Blant, S.; Hadjur, C.; Ballini, J. P.; Wagnières, G.; Fontolliet, C.; van den Bergh, H.; Monnier, P. Photodynamic Therapy of Early Squamous Cell Carcinoma with Tetra(m-Hydroxyphenyl)chlorin: Optimal Drug-Light Interval. *Br. J. Cancer* **1997**, *76* (8), 1021–1028.

(11) Houle, J.-M. H.; Strong, A. Clinical Pharmacokinetics of Verteporfin. *J. Clin. Pharmacol.* **2002**, *42* (5), 547–557.

(12) Huggett, M. T.; Jermyn, M.; Gillams, A.; Illing, R.; Mosse, S.; Novelli, M.; Kent, E.; Bown, S. G.; Hasan, T.; Pogue, B. W.; et al. Phase I/II Study of Verteporfin Photodynamic Therapy in Locally Advanced Pancreatic Cancer. *Br. J. Cancer* **2014**, *110* (7), 1698–1704.

(13) Saavedra, R.; Rocha, L. B.; Dabrowski, J. M.; Arnaut, L. G. Modulation of Biodistribution, Pharmacokinetics, and Photosensitivity with the Delivery Vehicle of a Bacteriochlorin Photosensitizer for Photodynamic Therapy. *ChemMedChem* **2014**, *9* (2), 390–398.

(14) Arnaut, L. G.; Pereira, M. M.; Dąbrowski, J. M.; Silva, E. F. F.; Schaberle, F. a; Abreu, A. R.; Rocha, L. B.; Barsan, M. M.; Urbańska, K.; Stochel, G.; et al. Photodynamic Therapy Efficacy Enhanced by Dynamics: The Role of Charge Transfer and Photostability in the Selection of Photosensitizers. *Chemistry* **2014**, *20* (18), 1–13.

(15) Kabingu, E. N. Photodynamic Therapy Mechanisms of Anti-Tumor Immunity, State University of New York at Buffalo, 2007.

(16) Mroz, P.; Hashmi, J. T.; Huang, Y.-Y.; Lange, N.; Hamblin, M. R. Stimulation of Anti-Tumor Immunity by Photodynamic Therapy. *Expert Rev. Clin. Immunol.* **2011**, *7* (1), 75–91.

(17) Garg, a D.; Martin, S.; Golab, J.; Agostinis, P. Danger Signalling during Cancer Cell Death: Origins, Plasticity and Regulation. *Cell Death Differ.* **2014**, *21* (1), 26–38.

(18) Panzarini, E.; Inguscio, V.; Dini, L. Immunogenic Cell Death: Can It Be Exploited in Photodynamic Therapy for Cancer? *Biomed Res. Int.* **2013**, *2013*.

(19) Rocha, L. B.; Gomes-da-Silva, L. C.; Dąbrowski, J. M.; Arnaut, L. G. Elimination of Primary Tumours and Control of Metastasis with Rationally Designed Bacteriochlorin Photodynamic Therapy Regimens. *Eur. J. Cancer* **2015**, *51*, 1822–1830.

(20) Marx, V. Tracking Metastasis and Tricking Cancer. *Nature* **2013**, *494*, 133–136.

(21) Shams, M.; Owczarczak, B.; Manderscheid-Kern, P.; Bellnier, D. a.; Gollnick, S. O. Development of Photodynamic Therapy Regimens That Control Primary Tumor Growth and Inhibit Secondary Disease. *Cancer Immunol. Immunother.* **2014**, *64* (3), 287–297.

(22) Ray, M. R.; Jablons, D. M. Hallmarks of Metastasis. In *Lung Cancer Metastasis*; Keshamouni, V., Arenberg, D., Kalemkerian, G., Eds.; Springer: New York, 2009; pp 29–46.

(23) Pulaski, B. a; Ostrand-Rosenberg, S. Reduction of Established Spontaneous Mammary Carcinoma Metastases Following Immunotherapy with Major Histocompatibility Complex Class II and B7.1 Cell-Based Tumor Vaccines. *Cancer Res.* **1998**, *58*, 1486–1493.

(24) Pulaski, B. A.; Ostrand-Rosenberg, S. Mouse 4T1 Breast Tumor Model. *Curr. Protoc. Immunol.* **2000**, *20.2*, 1–16.

(25) Pulaski, B. a.; Terman, D. S.; Khan, S.; Muller, E.; Ostrand-Rosenberg, S. Cooperativity of Staphylococcal Aureus Enterotoxin B Superantigen, Major Histocompatibility Complex Class II, and CD80 for Immunotherapy of Advanced Spontaneous Metastases in a Clinically Relevant Postoperative Mouse Breast Cancer Model. *Cancer Res.* **2000**, *60* (10), 2710–2715.

(26) Tao, K.; Fang, M.; Alroy, J.; Sahagian, G. G. Imagable 4T1 Model for the Study of Late Stage Breast Cancer. *BMC Cancer* **2008**, *8*, 228.

(27) DuPré, S. a.; Redelman, D.; Hunter, K. W. The Mouse Mammary Carcinoma 4T1: Characterization of the Cellular Landscape of Primary Tumours and Metastatic Tumour Foci. *Int. J. Exp. Pathol.* **2007**, *88* (5), 351–360.

(28) Gokcinar, D.; Ergin, V.; Cumaoglu, A.; Menevse, A.; Aricioglu, A. Effects of Ketamine, Propofol, and Ketofol on Proinflammatory Cytokines and Markers of Oxidative Stress in a Rat Model of Endotoxemia-Induced Acute Lung Injury. *Acta Biochim. Pol.* **2013**, *60* (3), 451–456.

(29) Nudp, E. K.; Ranjar, A.; Kharkhane, B.; Heidary, S. T.; Gharebaghi, Z. Antioxidative Effects of Propofol vs. Ketamin in Individuals Under-Going Surgery. *Arch. Iran. Med.* **2014**, *17* (7), 486–489.

(30) Bailey-Downs, L. C.; Thorpe, J. E.; Disch, B. C.; Bastian, A.; Hauser, P. J.; Farasyn, T.; Berry, W. L.; Hurst, R. E.; Ihnat, M. a. Development and Characterization of a Preclinical Model of Breast Cancer Lung Micrometastatic to Macrometastatic Progression. *PLoS One* **2014**, *9* (5), e98624.

(31) Henderson, B. W.; Gollnick, S. O.; Snyder, J. W.; Busch, T. M.; Kousis, P. C.; Cheney, R. T.; Morgan, J. Choice of Oxygen-Conserving Treatment Regimen Determines the Inflammatory Response and Outcome of Photodynamic Therapy of Tumors. *Cancer Res.* **2004**, *64* (6), 2120–2126.

(32) Jones, S. a. Directing Transition from Innate to Acquired Immunity: Defining a Role for IL-6. *J. Immunol.* **2005**, *175* (6), 3463–3468.

(33) Brackett, C. M.; Owczarczak, B.; Ramsey, K.; Maier, P. G.; Gollnick, S. O. IL-6 Potentiates Tumor Resistance to Photodynamic Therapy (PDT). *Lasers Surg. Med.* **2011**, *43* (7), 676–685.

(34) Lou, P.-J.; Jäger, H. R.; Jones, L.; Theodossy, T.; Bown, S. G.; Hopper, C. Interstitial Photodynamic Therapy as Salvage Treatment for Recurrent Head and Neck Cancer. *Br. J. Cancer* **2004**, *91* (3), 441–446.

(35) Svanberg, K.; Bendsoe, N.; Axelsson, J.; Andersson-Engels, S.; Svanberg, S. Photodynamic Therapy: Superficial and Interstitial Illumination. *J. Biomed. Opt.* **2011**, *15* (4), 041502.

(36) St Denis, T. G.; Aziz, K.; Waheed, A. a; Huang, Y.-Y.; Sharma, S. K.; Mroz, P.; Hamblin, M. R. Combination Approaches to Potentiate Immune Response after Photodynamic Therapy for Cancer. *Photochem. Photobiol. Sci.* **2011**, *10* (5), 792–801.

(37) Castano, A. P.; Mroz, P.; Wu, M. X.; Hamblin, M. R. Photodynamic Therapy plus Low-Dose Cyclophosphamide Generates Antitumor Immunity in a Mouse Model. *Proc. Natl. Acad. Sci. U. S. A.* **2008**, *105* (14), 5495–5500.

(38) Reginato, E.; Mroz, P.; Chung, H.; Kawakubo, M.; Wolf, P.; Hamblin, M. R. Photodynamic Therapy plus Regulatory T-Cell Depletion Produces Immunity against a Mouse Tumour That Expresses a Self-Antigen. *Br. J. Cancer* **2013**, *109* (8), 2167–2174.

(39) Chen, X.; Yang, Y.; Zhou, Q.; Weiss, J. M.; Howard, O. Z.; McPherson, J. M.; Wakefield, L. M.; Oppenheim, J. J. Effective Chemoimmunotherapy with Anti-TGFβ Antibody and Cyclophosphamide in a Mouse Model of Breast Cancer. *PLoS One* **2014**, *9* (1), 1–10.

(40) Chen, L.; Huang, T.-G.; Meseck, M.; Mandeli, J.; Fallon, J.; Woo, S. L. C. Rejection of Metastatic 4T1 Breast Cancer by Attenuation of Treg Cells in Combination with Immune Stimulation. *Mol. Ther.* **2007**, *15* (12), 2194–2202.

(41) Mroz, P.; Castano, A. P.; Hamblin, M. R. Stimulation of Dendritic Cells Enhances Immune Response after Photodynamic Therapy. *Biophotonics Immune Responses IV*. **2009**, 717803–717803 – 10.

Impact of Photodynamic Therapy with the photosensitizer redaporfin in distant metastasis

Ana C. S. Lobo*[1], Lígia C. Gomes-da-Silva[1], Célia M. Gomes[2] and Luis G. Arnaut[1]

[1] Chemistry Department, University of Coimbra, Rua Larga, 3004-535 Coimbra, Portugal

[2] IBILI, Faculty of Medicine, University of Coimbra, Azinhaga de Santa Comba, 3000-354 Coimbra, Portugal

SUPPLEMENTARY INFORMATION

Materials and Methods

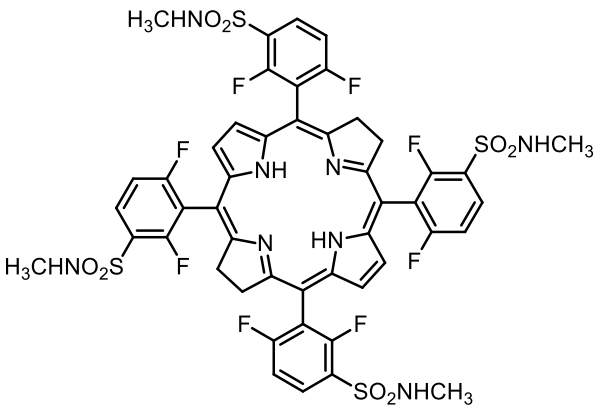

Figure S1. Molecular structure of 5,10,15,20-tetrakis(2,6-difluoro-3-N-ethylsulfamoylphenyl) bacteriochlorin (F_2BMet or redaporfin).

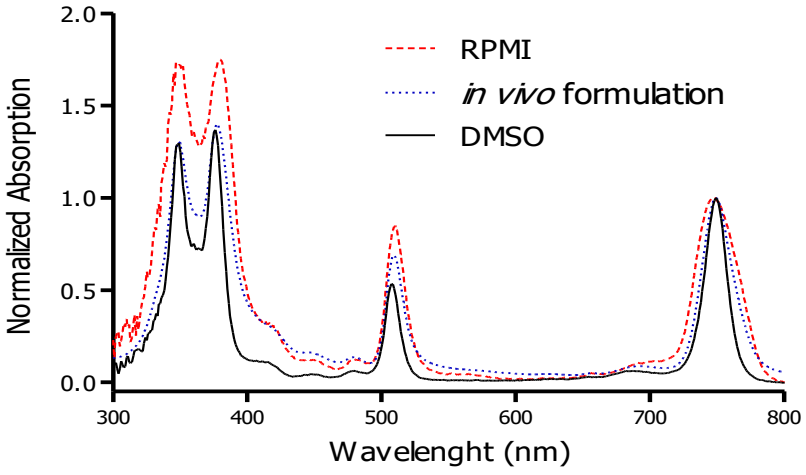

Graph S1. Spectra of normalized absorption of redaporfin in DMSO (black), RPMI (red) and *in vivo* formulation (blue).

Preparation of culture medium

For 1 L of RPMI medium, 10.4 g of RPMI-1640, 2.4 g of HEPES and 2 g of sodium bicarbonate were added to 890 mL of milli-Q water, 100 mL of heat-inactivated fetal bovine serum (FBS), and 10 mL of penicillin-streptomycin (PS). The mixture was stirred until a homogeneous solution was obtained. Solution was filtered, inside the laminar flow hood, through a filter with a porosity of 0.2 μm. All reagents were purchased from Sigma Life Sciences unless stated otherwise.

Preparation of phosphate buffer saline (PBS)

For 1 L of PBS, 0.2 g of potassium phosphate monobasic anhydrous (KH_2PO_4), 0.2 g potassium chloride (KCl), 1.15 g of sodium phosphate dibasic (Na_2HPO_4) and 0.4 g of sodium chloride (NaCl) were added to 1 L of milli-Q water. The mixture was stirred until a homogeneous solution was obtained and then was filtered, inside the laminar flow hood, through a filter with a porosity of 0.2 μm.

Measurement of absorbance

Absorbance spectra of redaporfin were recorded in UV-visible Recording Spectrophotometer (Shimadzu). The samples diluted from stock solutions were measured in quartz cuvettes with an optical path of 1 cm. All measurements were performed at room temperature. Concentration of redaporfin solution used for all experiments was calculated using Beer-Lambert Law: $A = \varepsilon\, l\, c$.

In vitro and in vivo formulations

For cellular assays, stock solutions of redaporfin were prepared in dimethyl sulfoxide (DMSO) (≈ 1-2 mM). For in vivo intravenous administrations, redaporfin was dissolved in 0.2 % Kolliphor, 1% ethanol and 98.8 % NaCl.

Measurement of cell viability by fluorescence – Alamar blue assay

Measurements of cytotoxicity were performed in 96-well plate using Alamar blue assay by fluorescence. After each experiment, cells were washed 3 times and was incubated with 0.01 mg/mL of Alamar blue diluted in the respective culture medium. After approximately 2 hours, cell viability was assessed by the assessed by fluorescence using a Synergy HT Multi-Mode Microplate Reader (BioTek), λ_{exc} = 560 nm and λ_{em} = 590 nm).

Preparation of anesthesia

For in vivo and in vitro studies, anesthesia was prepared with a mixture of ketamine and xylazine in a 5:1 ratio (v:v). 0.750 mL of ketamine (0.1 g/mL) and 0.250 mL (23.3 mg/ml) were added to 4 mL of phosphate buffer saline (PBS). Solution was filtered, inside the laminar flow hood, through a filter with a porosity of 0.2 μm.

Figure S2. PDT illumination procedure.

Data Results

Table S1 . Cytotoxicity data of in vitro PDT with redaporfin in 4T1 and 4T1-luc2 cell lines.

Redaporfin concentration (μM)	4T1 cell line					4T1-luc2 cell line				
	Cell viability (%)			Mean	SD	Cell viability (%)			Mean	SD
0.0781	106.51	98.16	111.11	105.26	6.57	106.95	102.09	95.48	101.51	5.76
0.156	98.05	92.49	104.17	98.24	5.84	98.94	101.22	96.93	99.03	2.14
0.3125	100.69	79.65	101.45	93.93	12.37	95.87	82.41	93.79	90.69	7.24
0.625	77.04	61.33	100.73	79.70	19.84	83.64	57.82	86.34	75.94	15.74
1.25	59.44	44.42	76.90	60.25	16.25	51.40	30.19	61.70	47.77	16.07
2.5	34.92	27.40	47.47	36.60	10.14	31.51	17.14	32.05	26.90	8.46
5	24.80	12.79	17.87	18.49	6.03	17.31	9.49	13.34	13.38	3.91
10	15.69	13.20	9.87	12.92	2.92	12.48	9.44	9.39	10.43	1.77

Table S2. IC50 values of in vitro PDT with redaporfin in 4T1 and 4T1-luc2 cell lines and data from statistical significance of cell lines differences, by the Student's t test at a P set at 0.05.

Cell line	*IC50 (μM)*			*Mean (μM)*	*SD (μM)*	*P value of student's t test*
4T1	1.2	0.8	2.0	1.3	0.36	0.6
4T1-luc2	1.1	0.6	1.6	1.1	0.27	

Table S3. Cytotoxicity data of in vitro PDT with redaporfin (5 μM) and different concentrations of anesthesia in 4T1 cell line.

Redaporfin: Anethesia (w:w)	Cell viability (%)			Mean	SD
1:0	32.68	16.23	9.22	19.38	12.05
1:1	32.93	17.88	9.65	20.15	11.81
1:5	20.13	10.38	9.42	13.31	5.93
1:10	10.34	8.95	9.46	9.58	0.71
1:20	9.90	8.53	9.40	9.28	0.69
1:30	9.31	8.72	9.47	9.17	0.39

Table S4. Statistical significance of data from Table S3 evaluated with the one-way ANOVA followed by Dunnett's Multiple Comparison test was performed at a P set at 0.05.

Dunnett's Multiple Comparison Test	Mean Diff.	q	Significant? P < 0.05?
1:0 vs 1:1	-0,7798	0,1306	No
1:0 vs 1:5	6,065	1,016	No
1:0 vs 1:10	9,792	1,640	No
1:0 vs 1:20	10,10	1,691	No
1:0 vs 1:30	10,21	1,710	No

Table S5. Dark cytotoxicity data of incubation with redaporfin (5 μM) and different concentrations of anesthesia in 4T1 cell line.

Redaporfin: Anethesia (w:w)	Cell viability (%)			Mean	SD
1:0	111.37	103.69	97.92	104.32	6.75
1:1	111.86	97.78	92.62	100.75	9.96
1:5	116.49	101.45	93.39	103.78	11.72
1:10	118.74	98.87	88.09	101.90	15.55
1:20	110.81	94.30	76.76	93.96	17.03
1:30	111.55	88.71	78.52	92.93	16.92

Table S6. Statistical significance of data from Table S5 evaluated with the one-way ANOVA followed by Dunnett's Multiple Comparison test was performed at a P set at 0.05.

Dunnett's Multiple Comparison Test	Mean Diff.	q	Significant? P < 0.05?
1:0 vs 1:1	3,573	0,3231	No
1:0 vs 1:5	0,5459	0,04938	No
1:0 vs 1:10	2,423	0,2192	No
1:0 vs 1:20	10,37	0,9377	No
1:0 vs 1:30	11,40	1,031	No

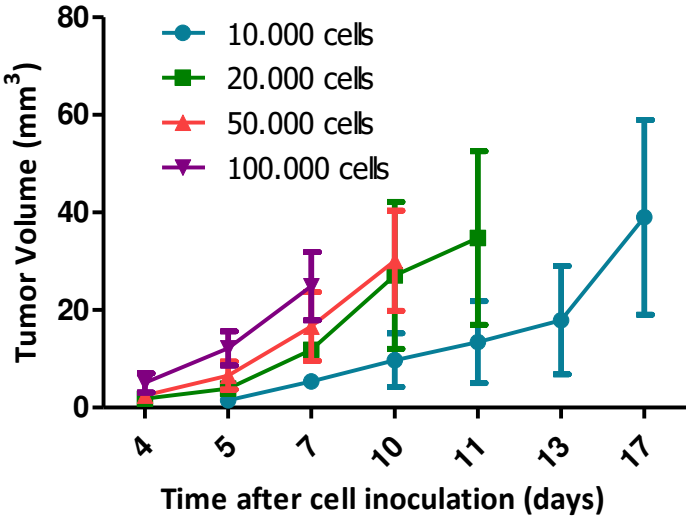

Graph S2. Tumor kinetics of 4T1 tumors inoculated with different number of cells for the metastatic model optimization. Tumors growth were followed until animals were submitted to surgery.

Figure S3. Animals submitted to surgery revealed no tumor regrowth, which was confirmed by bioluminescence imaging.

Figure S4. Imaging data from metastatic model optimization. 4 groups of animals (n=4) were inoculated with different concentration of inoculated cells, **1x10^4, 2x10^4, 5x10^4 and 1x10^{5}cells,** corresponding respectively to A, B, C and D groups in the following data. When the largest diameter of tumor attained 4 mm the animals were submitted to surgery and metastasis onset was assessed by imaging luminescence 27, 34 and 41 days after tumor inoculation.

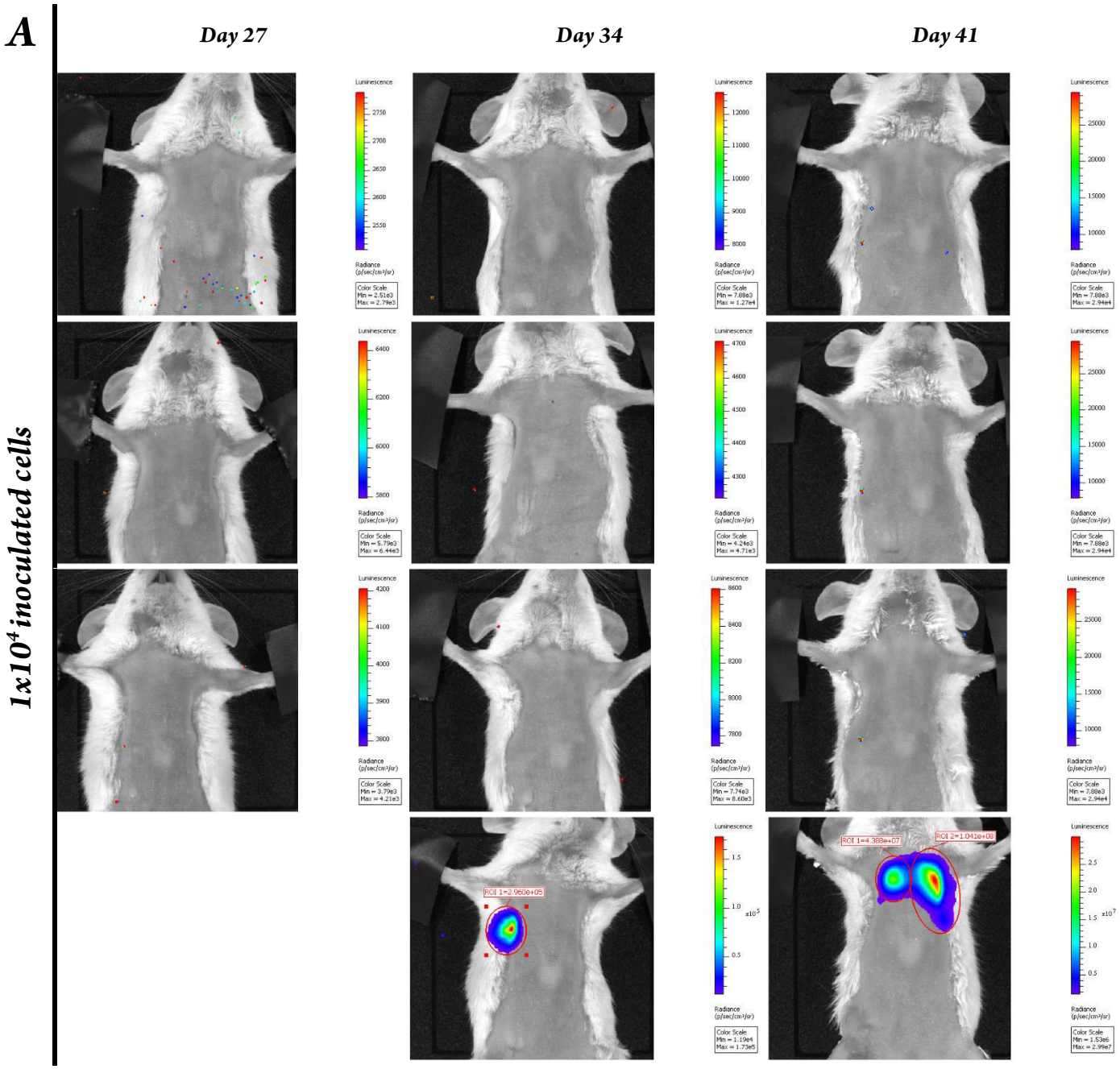

B

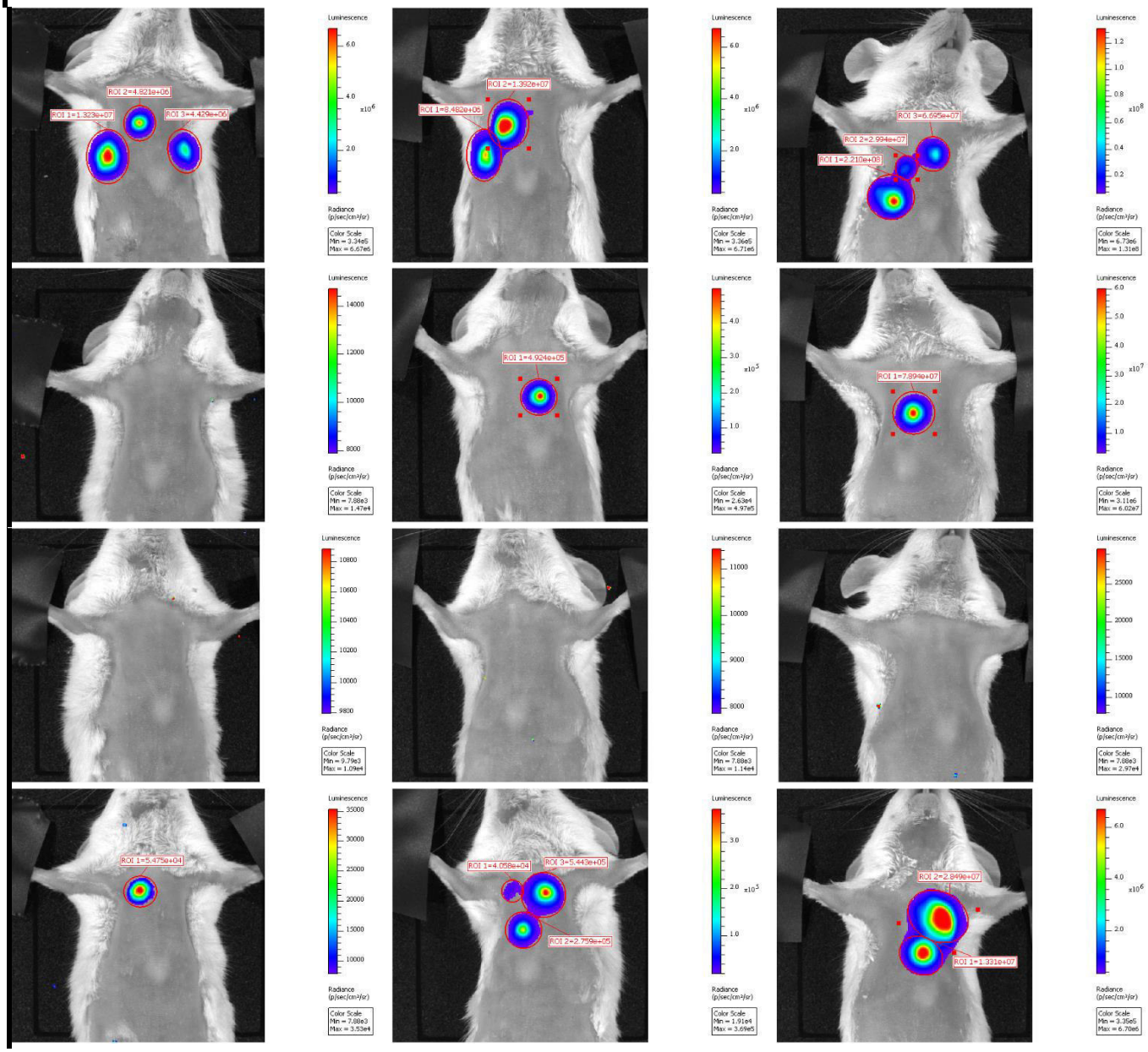
Day 27
Day 34
Day 41
2x10⁴ inoculated cells
ROI 1=1.323e+07
ROI 2=4.821e+06
ROI 3=4.429e+06
ROI 1=8.482e+05
ROI 2=1.392e+07
ROI 1=2.210e+06
ROI 2=2.994e+07
ROI 3=6.695e+07
ROI 1=4.924e+05
ROI 1=7.894e+07
ROI 1=5.475e+04
ROI 1=4.058e+04
ROI 3=5.443e+05
ROI 2=2.759e+05
ROI 1=1.331e+07
ROI 2=2.849e+07
Luminescence
Radiance (p/sec/cm²/sr)
Color Scale

C

5x10⁴ inoculated cells

Day 27 ***Day 34*** ***Day 41***

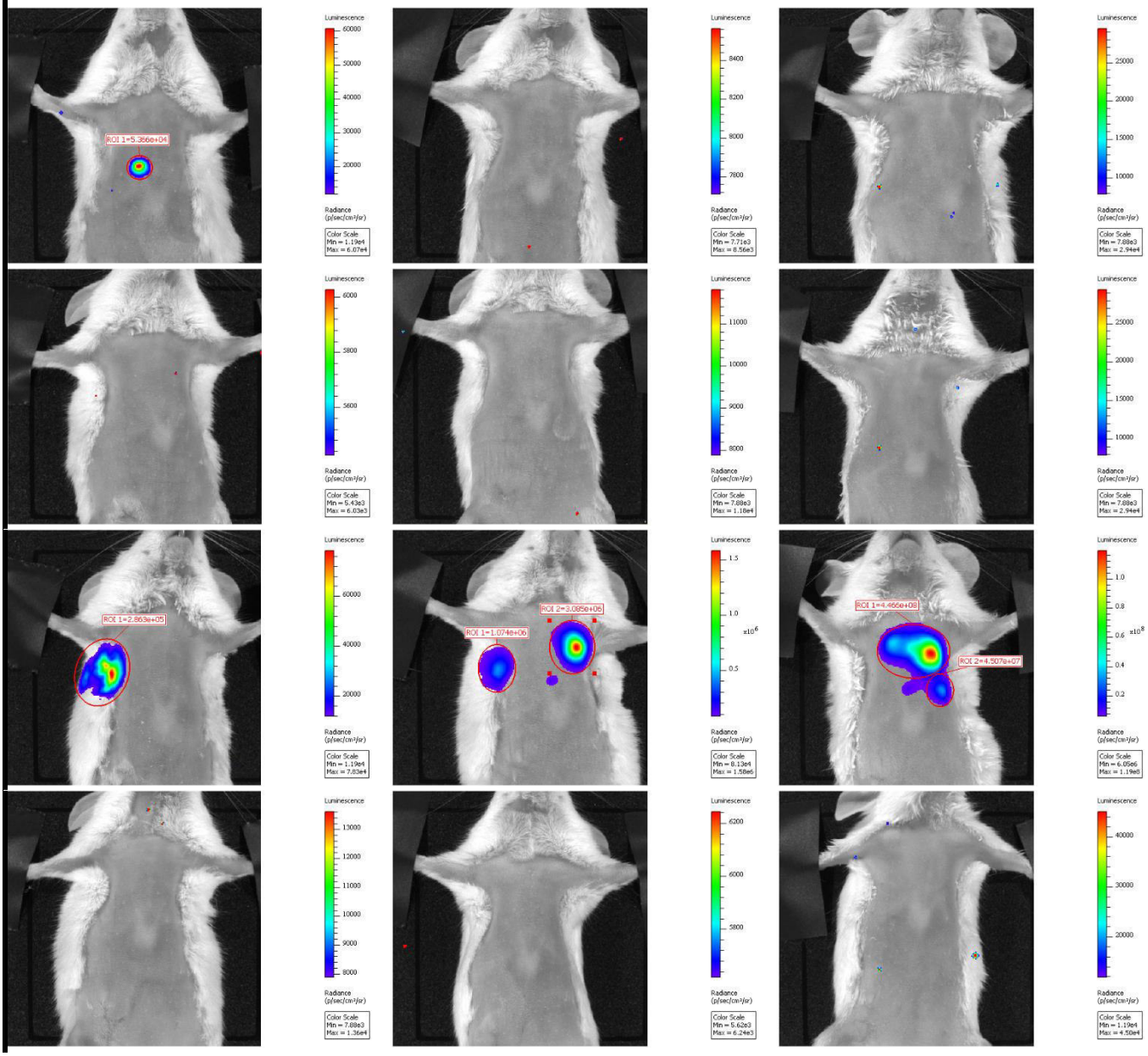

D

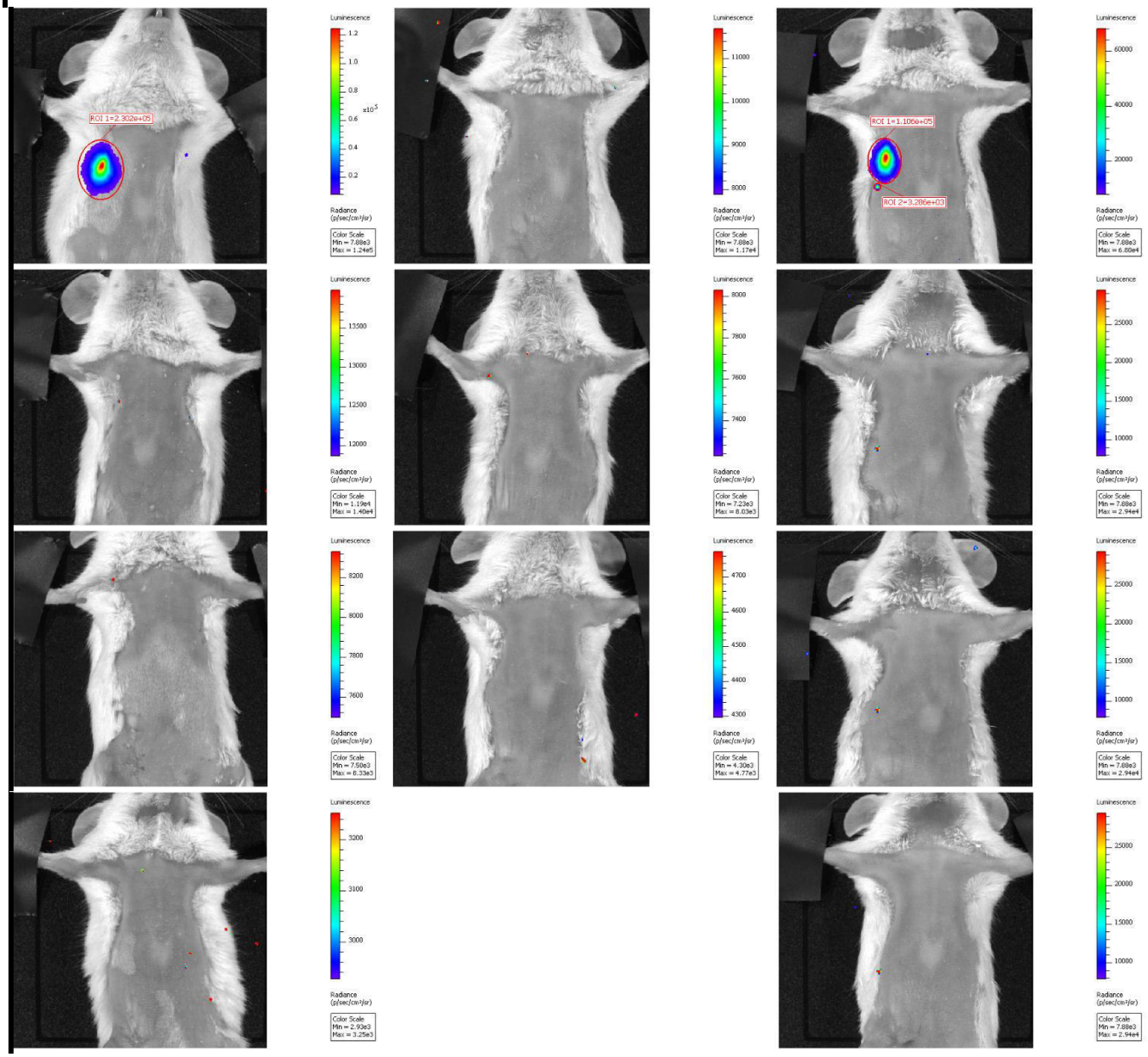

Table S7. Parameters characterization of the several PDT regimens for 4T1-luc2 orthotopic tumor illumination protocol optimization.

Protocol	N	Tumor diameter before PDT (mm)	Drug-to-light interval (DLI)(h)	Drug dose (mg/kg)	Light dose (J/cm²)	Laser Power (mW)	Fluence rate (mW/cm²)	Diameter (cm)	Survivals to the treatment (%)	Impact on the tumor
1	7	3 – 4	0.25	1.00	50	173	130	1.3	43	no impact
2	2	5	0.25	0.75	50	173	130	1.3	100	no impact
3	2	3 – 5	0.25	0.75	50	173	182	1.1	100	no impact
4	1	5	0.25	1.00	50	173	182	1.1	100	no impact
5	1	5	72	1.00	100	173	130	1.3	100	necrosis
6	1	5	72 & 0.25	1.00 & 0.5	80	173	130	1.3	0	-
7	1	3	72 & 0.25	1.00 & 0.5	60	173	130	1.3	100	no impact
8	4	4 - 5	24 & 0.25	1.00 & 0.5	50	173	220	1.0	0	-
9	3	5 - 6	144 & 72 & 0.25	1.00 & 1.00 & 0.4	50	173	220	1.0	100	necrosis
10	3	4	72 & 0.25	2.00 & 0.4	50	173	220	1.0	0	-
11	6	4	72	2.00	50	173	220	1.0	100	edema
12	6	4	72	2.00	75	103	130	1.0	0	edema and necrosis
13	6	3	72	2.00	65	103	130	1.0	0	edema

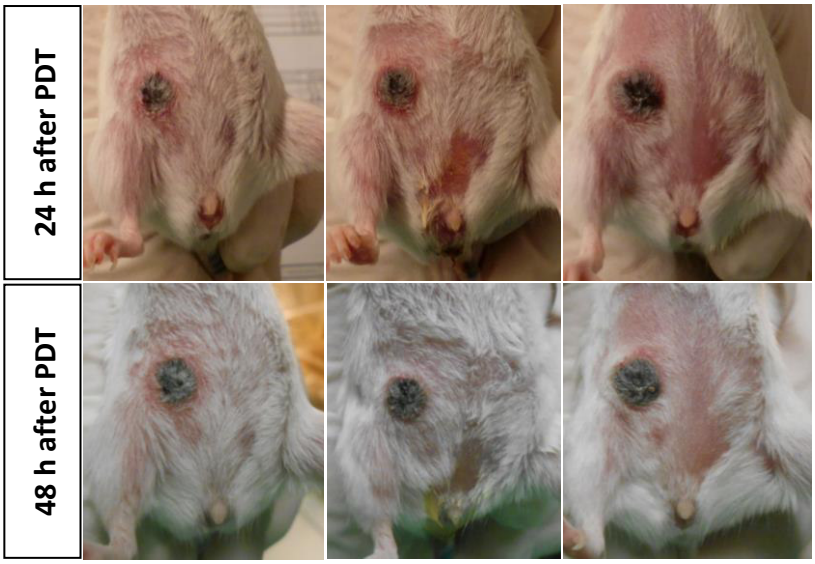

Figure S5. Impact of PDT protocol 9 in 4T1 tumors. After 72 h tumors started to regrow.

Table S8. Tumor volumes (mm^3) of animals from protocols described in Table S7. Until protocol 7, the number of 4T1-luc2 inoculated cells was $2x10^5$, because the metastatic model was still not optimized. From this, the number of inoculated cells was $2x10^4$ cells.

Protocol 1							
Day	**4**	**5**	**7**	**11**	**14**	**18**	**21**
1	6.3	28.2	18.7				
2	12.0	8.1	13.9				
3	7.5	14.9	16.2	28.2	40.6	66.0	134.5
4	4.9	5.6	13.0	18.4	78.0	107.9	171.4
5	6.3	6.8	24.0				
6	6.9	18.0	21.4				
7	9.5	14.9	29.6	49.4	101.3	148.1	175.1
Mean	7.6	13.8	19.5	32.0	73.3	107.3	160.3
SD	2.4	7.9	5.9	15.8	30.6	41.1	22.4

Protocol 2								
Day	**22**	**25**	**27**	**28**	**29**	**32**	**34**	**36**
1	9.1	24.0	51.9					
2	5.4	20.7	39.0	117.2	67.6	67.6	128.4	285.4
Mean	7.3	22.3	45.4					
SD	2.6	2.3	9.1					

Protocol 3										
Day	**18**	**22**	**25**	**27**	**28**	**29**	**32**	**34**	**36**	**40**
1	4.6	6.7	10.5	7.4	8.4	11.3	13.0	17.4	28.2	97.2
2	3.4	15.3	36.5	55.2	65.6	76.2	100.9	186.5	184.7	344.4
Mean	4.0	11.0	23.5	31.4	37.0	43.8	57.0	102.0	106.6	220.8
SD	0.9	6.0	18.3	33.8	40.4	45.9	62.1	119.6	110.9	174.8

Protocol 4											
Day	**15**	**18**	**22**	**25**	**27**	**28**	**29**	**32**	**34**	**36**	**40**
1	9.8	9.5	26.6	51.9	107.9	102.9	124.5	172.5	233.3	251.9	499.9

Table S8 continuation. Tumor volumes (mm^3) of animals from protocols described in Table S7. Until protocol 7, the number of 4T1-luc2 inoculated cells was $2x10^5$, because the metastatic model was still not optimized. From this, the number of inoculated cells was $2x10^4$ cells.

Protocol 5		
Day	**6**	**10**
1	18.3	41.8

Protocol 6			
Day	**3**	**6**	**10**
1	2.7	19.7	42.9

Protocol 7	
Day	**10**
1	6.9

Protocol 8				
Day	**6**	**9**	**13**	**16**
1	18.5	22.4	48.8	48.8
2	22.4	26.4	61.1	80.0
3	14.3	19.6	52.0	55.4
4	9.0	26.9	55.4	68.1
Mean	16.0	23.8	54.3	63.1
SD	5.0	3.0	4.6	12.0

Protocol 9								
Day	**4**	**7**	**11**	**12**	**15**	**18**	**19**	**25**
1	2.5	14.9	39.7	39.8	72.9	120.8	120.8	368.5
2	1.5	10.5	24.0	35.3	42.5	70.2	74.4	231.2
3	2.8	15.9	40.7	51.6	70.3	117.2	109.8	285.4
Mean	2.3	13.8	34.8	42.2	61.9	102.8	101.7	295.0
SD	0.6	2.9	9.4	8.4	16.8	28.2	24.3	69.2

Protocol 10							
Day	**4**	**6**	**7**	**9**	**10**	**11**	**12**
1	3.0	13.3	14.9	21.0	28.7		
2		4.0	6.9	11.7		18.4	25.1
3	6.3	6.8	11.2	10.1	17.7		
Mean	4.7	8.0	11.0	14.2	23.2		
SD	2.3	4.8	4.0	5.9	7.8		

Protocol 11								
Day	**6**	**8**	**10**	**13**	**14**	**16**	**20**	**23**
1	6.8	7.8	12.1		27.8	40.4	83.8	163.7
2	4.2	6.1	12.6	25.3		31.0	63.6	175.7
3	9.7	14.5	29.5		44.5	73.7	219.3	338.7
4	3.7	7.8	13.5	37.0		34.7	150.0	199.1
5	5.1	12.0	12.8		43.2	46.7	130.5	220.5
6	5.3	7.5	12.5	31.2		29.2	104.4	122.8
Mean	5.8	9.3	15.5	31.1	38.5	42.6	125.3	203.4
SD	2.2	3.3	6.9	5.9	9.3	16.5	55.6	74.1

Table S8 conclusion. Tumor volumes (mm^3) of animals from protocols described in Table S6.

Protocol 12						
Day	**6**	**7**	**10**	**13**	**14**	**17**
1	1.4		5.1	16.3	18.9	34.2
2	3.5	5.0	10.9	31.9	42.5	
3	3.4	6.1	19.5	38.8	42.5	
4	5.1	7.8	11.5	36.1	36.0	
5	4.2	8.4	19.1	40.7	46.5	
6	9.5	11.6	24.5	44.5	43.7	
Mean	4.5	7.8	15.1	34.7	38.4	
SD	2.7	2.5	7.1	10.0	10.1	

Protocol 13				
Day	**6**	**7**	**10**	**13**
1	2.1	2.8	4.2	16.9
2	0.0	3.6	5.6	9.0
3	2.3	4.2	5.6	14.4
4	1.8	5.8	6.6	17.2
5	2.3	7.5	9.5	18.4
6	1.5	6.0	7.1	15.8
Mean	1.7	5.0	6.4	15.3
SD	0.9	1.8	1.8	3.3

This master project has resulted in one oral communication at II Young Researchers Symposium of the Spanish Society of Medicinal Chemistry (12th June 2015, Madrid, Spain) and one poster presentation at XXIV Encontro Nacional da Sociedade Portuguesa de Química (1st-3rd July 2015, Coimbra, Portugal). The poster is presented below.

IMPACT OF PDT WITH REDAPORFIN IN DISTANT METASTASES

Ana C. S. Lobo[1], Lígia C. Gomes-da-Silva[1], Célia M. Gomes[2], Luís G. Arnaut[1]

[1] Department of Chemistry, University of Coimbra, Portugal. catarinalobo13@gmail.com
[2] IBILI, Faculty of Medicine, University of Coimbra, Portugal

Introduction

Metastatic diseases are the main cause of death of cancer patients. Thus, treating cancer disease requires therapies capable of treating primary tumors but also able to eradicate distant secondary diseases [1]. Photodynamic therapy (PDT) with redaporfin has revealed promising results, with high percentage of cures of subcutaneous tumors along with the ability to stimulate the immune system [2].
Our purpose is to develop a protocol for an animal model (BALB/c mice with orthotopic 4T1 mammary carcinoma tumor) that can be used to compare surgery against PDT in the elimination of the primary tumor and the control of metastases.

Materials and Methods

Chemicals: 5,10,15,20-Tetrakis(2,6-difluoro-3-N-methylsulfamoylphenyl)bacteriochlorin (redaporfin) was recently described [3]. Luzitin SA (Coimbra, Portugal) provided redaporfin as a powder in a sealed amber glass vial under N_2 atmosphere.

Cell Culture: 4T1-luc2 cell line were obtained from Perkin Elmer and were cultured in RPMI medium 1640 supplemented with 10% fetal bovine serum and 1% penicillin/streptomycin at 37° C.

Mouse Tumor Model: The animals in these studies were female BALB/c mice (Charles River Laboratories®, Barcelona, Spain) with 8 to 10 weeks of age, weighing 18-23 grams. For the tumor establishment different number of 4T1-luc2 cells were taken up in 0,05 mL of RPMI without serum and antibiotics ($1x10^4$, $2x10^4$, $5x10^4$ and $10x10^4$ cells) and were inoculated in the right abdominal mammary gland of each animal. The tumors were treated 7-11 days after the inoculation when the large diameter of the tumor reaches 4-5 mm. Control animals are subjected to surgery.

PDT regimens: Tumors illumination protocols described in Table 1 used an Omicron laser which was handled close to the surface of the tumor with a specific diameter of the laser spot. Tumor dimensions were determined before the illumination and then twice a week until the largest diameter attained 10 mm, at which point animal are sacrificed.

***In vivo* luminescence imaging:** Detection of metastases by imaging was performed with an IVIS Lumina XR (Xenogen Corporation-Caliper). After the mice were anesthetized with 150 μL of a ketamine/xylazine mixture (5:1), 100 μL of D-luciferin potassium salt (30 mg/mL) were intraperitoneally injected to the mice 5 minutes prior to imaging acquisition. Metastasization was monitored by bioluminescent imaging between days 27 and 41, and then the animals were sacrificed.

Results

The first detection of metastases in the animals subjected to surgery was observed 27 days after inoculation.
The higher percentage of metastasization corresponded to the inoculation of $2x10^4$ cells.

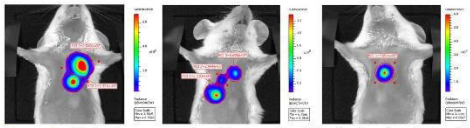

Figure 1. Bioluminescence imaging on day 41 of mice treated with surgery ($2x10^4$ inoculated cells).

Table 1. Studies of PDT regimens for tumor illumination protocol optimization.

Protocol	DLI	PDT Model	Drug dose (mg/Kg)	Light dose (J/cm²)	Spot diameter (cm)	Survivals to the treatment (%)	Impact on the tumor
1	15 min	vascular	1.00	50	1.3	43	no impact
2	15 min	vascular	0.75	50	1.3	100	no impact
3	15 min	vascular	0.75	50	1.1	100	no impact
4	15 min	vascular	1.00	50	1.1	100	no impact
5	72h	cellular	1.00	100	1.3	100	necrosis
6	72h & 15 min	cellular & vascular	1.00 & 0.5	80	1.3	0	-
7	72h & 15 min	cellular & vascular	1.00 & 0.5	60	1.3	100	no impact
8	24h & 15min	cellular & vascular	1.00 & 0.5	50	1.0	0	-
9	144h & 72h & 15 min	cellular & vascular	1.00 & 1.00 & 0.4	50	1.0	100	necrosis
10	72h & 15 min	cellular & vascular	2.00 & 0.4	50	1.0	0	-
11	72h	cellular	2.00	50	1.0	100	edema

Figure 2. Impact of PDT protocol 9, described in Table 1: A - before PDT; B - 24h after PDT; C - 48h after PDT. Tumor regrow 72h after PDT.

Conclusions

The inoculation of a smaller number of cells facilitates the metastasization process, as described in literature [4].
The resistance of 4T1 cells and the location of the tumor are a challenge to PDT. Tumor kinetics, timing of surgery and PDT treatment parameters still need to be optimized to obtain an effective treatment of the primary tumor and to evaluate the impact of the treatment in metastases.

Acknowledgements

The Coimbra Chemistry Center is supported by the Fundação para a Ciência e a Tecnologia (FCT), Portuguese Agency for Scientific Research, through the project PTDC/QUI-QUI/120182/2010 and the project PEst-OE/QUI/UI0313/2014. We thank Luzitin SA for the gift of redaporfin.

References

[1] Shams, M.; Owczarczak, B.; Manderscheid-Kern, P.; Bellnier, D.; Gollnick, S. Cancer Immunol, Immunother **2015,** 64(3):287-297.
[2] Rocha, L.; Gomes-da-Silva, L.; Dabrowski, J. M.; Arnaut, L. G. Eur. J. Cancer, **2015**.
[3] Arnaut, L.; Pereira, M.; Dabrowski, J.; Silva, E.; Schaberle, F.; Abreu, A.; Rocha, L. et al. Chem Eur J, **2015**, 20:5346-5357.
[4] Bailey-Downs, L.; Thorpe, J.; Disch, B.; Bastian, A.; Hauser, P. et al. PLoS ONE, **2014**, 9(5):e98624.